Algorithmic identification of the reactions that support or oppose the development of explosive modes in *n*-heptane/air autoignition

Dimitris M. Manias, *Efstathios Al. Tingas*, *Dimitris A. Goussis*[*]

Department of Mechanics, School of Applied Mathematics and Physical Sciences, National Technical University of Athens, 157 73 Athens, Greece

Abstract

The dynamics of two stage adiabatic auto-ignition of a homogeneous *n*-heptane/air mixture at constant volume is analyzed algorithmically, using the Computational Singular Perturbation (CSP) method. The fast dynamics of this reactive system become exhausted, while the slow dynamics is characterized by time scales that are of explosive character; i.e. the components of the system that generate these scales tend to lead the system away from equilibrium. The reactions that are responsible for the generation of these time scales and the species that relate with the explosive modes are identified with CSP-tools.

Introduction

Reactive systems introduce a wide range of time scales, the fastest of which are of dissipative character and tend to constrain the evolution of the system along a slow invariant manifold (SIM). Sometimes, the dynamics of the slow system that drives the process along the SIM is characterized by slow time scales that are of explosive character; i.e., time scales that characterize the movement of the system away from equilibrium. Such a situation arises in autoignition processes (Kazakov et al., 2006; Lu et al., 2010; Najm et al., 2010; Gupta et al., 2011), while in flames these explosive time scales need not be present, since diffusion is the main mechanism for initiating the reaction process in the fresh mixture (Lee et al., 2005).

Here, the autoignition process of a homogeneous *n*-heptane/air mixture will be considered. This system has been studied extensively by various researchers (Yoo et al., 2011; Shan et al., 2012; Gupta et al., 2013). In these studies the emphasis was placed in the identification of the reactions that influence the impact of the modes that associate to the explosive time scales. Here, the reactions that promote or oppose the generation of the explosive time scale that characterizes autoignition will be identified for the adiabatic autoignition of a homogeneous *n*-heptane/air mixture at $T_0 = 800$ K and $p_0 = 30$ atm, using the *Computational Singular Perturbation* (CSP) algorithm (Lam and Goussis, 1988, 1991). A preliminary analysis of this system was presented in Ref. (Diamantis et al., 2009).

It will be shown that as the autoignition process evolves, the nature of the reactions responsible for the generation of the characteristic explosive time scale evolves as well; starting from isomerization reactions and ending with reactions related to the hydrogen chemistry.

The Physical Problem

We consider adiabatic autoignition at constant volume of a homogeneous stoichiometric *n*-heptane/air mixture. The chemical kinetics mechanism employed here is the V.3.1 mechanism (n-heptane, 2012; Mehl et al., 2011), which consists of $N = 654$ species, $E = 6$ elements (C, H, N, O, Ar and He) and $K = 2827$ elementary reactions. Here, the forward and backward directions of the K elementary reactions will be considered as separate unidirectional reactions, so that the governing equations for the species mass fraction and temperature become:

$$\frac{d\mathbf{y}}{dt} = \frac{1}{\rho}\mathbf{W}\cdot\sum_{k=1}^{2K}\mathbf{S}_k R^k \tag{1}$$

$$\frac{dT}{dt} = \frac{1}{\rho c_v}\left(-\mathbf{h}_c\cdot\mathbf{W} + RT\mathbf{U}\right)\cdot\sum_{k=1}^{2K}\mathbf{S}_k R^k = \sum_{k=1}^{2K} e_k R^k \tag{2}$$

where $\mathbf{y}$ is the N-dim. state column vector of the species' mass fraction, $\mathbf{S}_k$ and R^k represent the stoichiometric vector and reaction rate, respectively, of the k-th unidirectional reaction, ρ is the mixture density, $\mathbf{W}$ is a $N \times N$ diagonal matrix with the species' molecular

[*]Corresponding author: dagoussi@mail.ntua.gr

weights in the diagonal, c_v is the heat capacity, $\mathbf{h}_c$ is the N-dim. vector of the species' absolute enthalpies, T is the temperature, R is the universal gas constant and $\mathbf{U} = [1,\ 1, \ldots,\ 1]$ (Williams, 1985; Law, 2006).

The Reduced Model according to CSP

In order to construct a reduced model, Eqs. (1) and (2) are cast in the form of the $(N+1)$-dim. system:

$$\frac{d\mathbf{z}}{dt} = \mathbf{g}(\mathbf{z}) = \sum_{k=1}^{2K} \hat{\mathbf{S}}_k R^k = \sum_{n=1}^{N-E+1} \mathbf{a}_n f^n \qquad (3)$$

where $\mathbf{z}$ is the $(N+1)$-dim. state column vector, defined as $\mathbf{z} = [\mathbf{y}, T]^T$, $\mathbf{a}_n$ is the $(N+1)$-dim. CSP column basis vector of the n-th mode and f^n is the related amplitude:

$$f^n = \mathbf{b}^n \cdot \mathbf{g}(\mathbf{z}) = \sum_{k=1}^{2K} \left(\mathbf{b}^n \cdot \hat{\mathbf{S}}_k\right) R^k \qquad (4)$$

and $\mathbf{b}^i \cdot \mathbf{a}_j = \delta^i_j$ (Lam and Goussis, 1988, 1994). The amplitudes f^{N-E+2} to f^{N+1} represent the conservation of the E elements, therefore, they are by definition zero. In order to preserve the orthogonality condition, the non-zero amplitudes $[f^1, ..., f^{N-E+1}]$ are set positive, by properly adjusting the sign of the $(N+1)$-dim. row vectors $\mathbf{b}^n$ (and therefore the sign of $\mathbf{a}_n$).

Assuming that the system in Eq. (3) exhibits M time scales that are of dissipative nature and much faster than the rest ($\tau_1 < \cdots < \tau_M << \tau_{M+1} < \cdots < \tau_{N-E+1}$), yields:

$$f^m \approx 0 \quad (m = 1, M) \qquad \frac{d\mathbf{z}}{dt} \approx \sum_{n=M+1}^{N-E+1} \mathbf{a}_n f^n \qquad (5)$$

The first of these two relations is an algebraic M-dim. system and defines the SIM, while the second is an $(N+1)$-dim. system of ODEs that governs the slow evolution of the process on the SIM. The evolution of Eq. (5) is free of the fast time scales (τ_1 to τ_M), so that its dynamics are characterized by the fastest of the slow time scales. The identification and analysis of the slow characteristic time scales, explosive or dissipative, is allowed by the availability of this equation (Trevino, 1989; Sanchez et al., 1997; Peters et al., 2002).

The CSP Tools

The time scales of the system are approximated by the relation $\tau_n = |\lambda_n|^{-1}$ $(n = 1, N-E+1)$, where λ_n is the n-th non-zero eigenvalue of the Jacobian $\mathbf{J}$ of $\mathbf{g}(\mathbf{z})$. This eigenvalue is defined as $\lambda_n = \boldsymbol{\beta}^n \cdot \mathbf{J} \cdot \boldsymbol{\alpha}_n$, where $\boldsymbol{\alpha}_n$ and $\boldsymbol{\beta}^n$ are the n-th right (column) and left (row), respectively, eigenvectors of $\mathbf{J}$. Taking into account the fact that the vector field $\mathbf{g}(\mathbf{z})$ is the sum of $2K$ terms, the n-th eigenvalue can be expressed as:

$$\lambda_n = \boldsymbol{\beta}^n \cdot \sum_{k=1}^{2K} grad\left(\hat{\mathbf{S}}_k R^k\right) \cdot \boldsymbol{\alpha}_n = c_1^n + ... + c_{2K}^n \qquad (6)$$

since $\mathbf{J} = grad(\hat{\mathbf{S}}_1 R^1) + \cdots + grad(\hat{\mathbf{S}}_{2K} R^{2K})$ (Goussis and Skevis, 2005). The magnitude of the terms c_k^n is indicative of the contribution of the k-th reaction to the n-th eigenvalue. Considering the case where λ_n is real (the extension to the case where some of the eigenvalues are complex pairs is straightforward (Goussis and Najm, 2006)), then, the c_k^n terms can be either positive or negative; positive (negative) c_k^n implies that the k-th reaction contributes to the explosive (dissipative) character of the n-th time scale τ_n. Naturally, when the positive (negative) terms outweigh the negative (positive) ones the n-th time scale is an explosive (dissipative) one.

The decomposition in fast/slow processes of the vector field $\mathbf{g}(\mathbf{y})$ allows the acquisition of significant physical understanding of complex chemical systems and it is possible by the use of CSP-related algorithmic tools. In particular, the contribution of each of the $2K$ reactions to the time scale τ_n can be assessed through the related term in Eq. (6), by employing the *Time scale Participation Index* (TPI):

$$J_k^n = \frac{c_k^n}{|c_1^n| + ... + |c_{2K}^n|} \qquad (7)$$

where $n = 1, N-E+1$, $k = 1, 2K$ and by definition $\sum_{k=1}^{2K} |J_k^n| = 1$ (Goussis and Skevis, 2005; Goussis and Najm, 2006). J_k^n measures the relative contribution of the k-th reaction to the n-th eigenvalue λ_n and, therefore, to the time scale τ_n.

Similarly, the relation of the n-th mode to the k-th component (mass fraction) of $\mathbf{z}$ can be assessed by employing the *CSP Pointer* (Po), defined as:

$$\mathbf{D}^n = diagn[\mathbf{a}_n \mathbf{b}^n] = [a_n^1 b_1^n, ..., a_n^{N+1} b_{N+1}^n] \qquad (8)$$

where, by definition $\sum_{k=1}^{N} a_n^k b_k^n = 1$ (Goussis and Skevis, 2005; Goussis and Najm, 2006). The magnitude of $D_k^n = a_n^k b_k^n$ measures the relation of the n-th mode to the k-th component of $\mathbf{z}$.

In the following the TPI and Po tools will be employed in order to investigate the explosive modes that develop during the autoignition process of the n-heptane/air mixture. The TPIs will identify reactions that contribute to the development of the explosive time

scale, say τ_e, which sets the time frame of the explosive mode's action. In contrast, the Pos will identify the variables (mass fractions or the temperature) that (i) are being affected the most by the explosive time scale, τ_e, and (ii) are functional in the reaction rates that have a significant presence in the expression of the amplitude f^e of the explosive mode.

Autoignition Dynamics of *n*-heptane/air Mixture

The explosive timescales that develop during the autoignition of a stoichiometric *n*-heptane/air mixture are displayed in Fig. 1 with red color. The temperature profile, displayed with black color, is superimposed on Fig. 1. It is shown that the explosive time scales (one fast and one slow) appear from the start of the process until the point where temperature undergoes a steep increase. This period will be referred as the *explosive stage*. In addition, the fastest of the explosive time scales will be denoted by $\tau_{e,f}$ and the slowest will be denoted by $\tau_{e,s}$.

An interesting feature exhibited in Fig. 1 is that from the start of the process $\tau_{e,f}$ is practically constant, while $\tau_{e,s}$ rapidly loses its explosive character and regains it shortly after, constantly accelerating in a steady rate till the point in time that it finally meets $\tau_{e,f}$ at $t = 0.00056$ s. As soon as they meet, both $\tau_{e,f}$ and $\tau_{e,s}$ for a short period. Fig. 1 shows that the point where $\tau_{e,f}$ and $\tau_{e,s}$ meet and the disappear is at the start of the *first stage* of autoignition.

The two explosive time scales re-appear at $t = 0.00063$ s. The fastest $\tau_{e,f}$ keeps accelerating and then decelerates rapidly on its way to meet for a second time $\tau_{e,s}$ at at $t = 0.00079$ s. Again, as soon as $\tau_{e,f}$ and $\tau_{e,s}$ meet they disappear. Figure 1 shows that this point now is at the start of the *second stage* of autoignition.

Diagnostics

Here, the origin of $\tau_{e,f}$ will be discussed, since it is the time scale that characterizes the process. Values of the related TPI and Po will be reported at the three points during the autoignition process, indicated by solid black bullets in Fig. 1. These points (P_1, P_2, P_3) refer to three key points of the process; the starting point, the point where $\tau_{e,f}$ reappears and the point where $\tau_{e,f}$ is the fastest.

The reactions with the largest values of TPI for the generation of $\tau_{e,f}$, as well as the species/variables with the largest Po at the points P_1-P_3, are displayed in Fig. 2.

At $t = 0$ (point P_1), Fig. 2 shows that the major contributors to the generation of $\tau_{e,f}$ are (i) intramolecular isomerization reactions of RO_2 to $QOOH$ (where R denotes C_nH_{2n+1} and Q denotes C_nH_{2n} groups) (ii) reactions of peroxyalkylhydroperoxides ($QOOH - O_2$) forming ketohyperoxides and OH, in agreement with Diamantis et al. (2009). This latter step is particularly significant because it initiates the preparation of the OH pool, which will be very important for the dynamics at later times (see Fig. 3(c)).

The reactions that oppose the generation of $\tau_{e,f}$ at $t = 0$ are dissociation reactions of RO_2 that lead to the formation of Q and HO_2. In addition, the CSP Pointer identifies RO_2 and $QOOH$ species as those that are mostly related to the development of $\tau_{e,f}$, which is reasonable considering that all of them are involved as reactants in the reactions with the largest TPI. These results are in full agreement with the evolution of the species' mass fractions of heptane isomers, as shown in Fig. 3(a).

As the autoignition process evolves, the reactions that contribute the most to the generation of $\tau_{e,f}$ retain almost constant values of TPI up to the start of the *first stage*. This is anticipated, since $\tau_{e,f}$ remains practically constant during that period. In this first stage, the heptane chemistry dominates, until the first temperature raise, where these higher molecules decomposite to C_1-C_3 chemistry lighter ones; see Fig. 3(b).

At the initiation of the *second stage*, where $\tau_{e,f}$ and $\tau_{e,s}$ re-appear, it is demonstrated by the CSP data for point P_2 in Fig. 2, that $\tau_{e,f}$ is characterized mainly by the chain branching reaction $H_2O_2(+M) \rightarrow OH + OH(+M)$, through which the hydrogen peroxide decomposes to the highly reactive hydroxyl radicals, thus contributing significantly to the creation of the necessary radical pool, as stated above. The action of this reaction is assisted by some C_1-C_3 reactions (Fig. 3(b)) that result either in the formation of OH/H_2O_2 (Fig. 3(c)) or unstable radicals. Since at point P_2 the temperature has already risen around 200 K and keeps rising, it can be concluded that this point lies in the thermal runway regime. As a result, it is fully reasonable the fact that the CSP Pointer has identified the temperature as the dominant variable that is mostly related to $\tau_{e,f}$.

As shown in Fig. 1, the acceleration of $\tau_{e,f}$ stops at point P_3, where $\tau_{e,f}$ reaches its minimum value. From that point and on, it starts a steep deceleration till it meets $\tau_{e,s}$ shortly afterwards. Both the results in Fig. 2 and the species' mass fraction of Fig. 3(c) suggest that the H_2/O_2 chemistry is now dominating the generation of $\tau_{e,f}$ with CO to CO_2 conversion providing a minor contribution. The reaction contributing the most to $\tau_{e,f}$ is the chain branching reaction $H + O_2 \rightarrow O + OH$. This

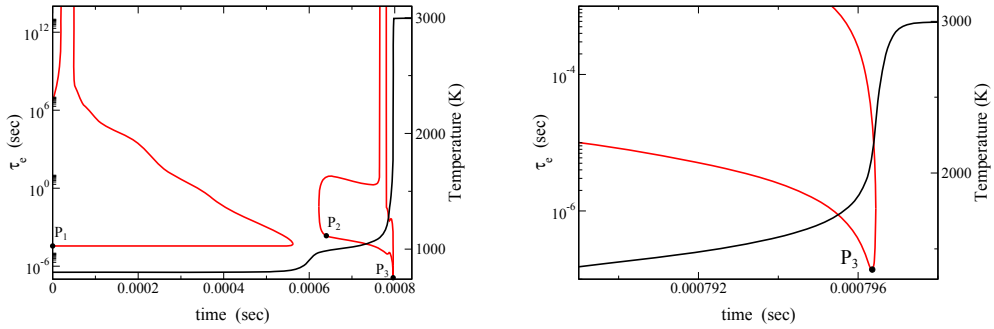

Figure 1: The evolution of the developing explosive timescales (red line) and temperature (black line) as a function of time: $P_0 = 30$ atm, $T_0 = 800$ K and $\phi = 1$.

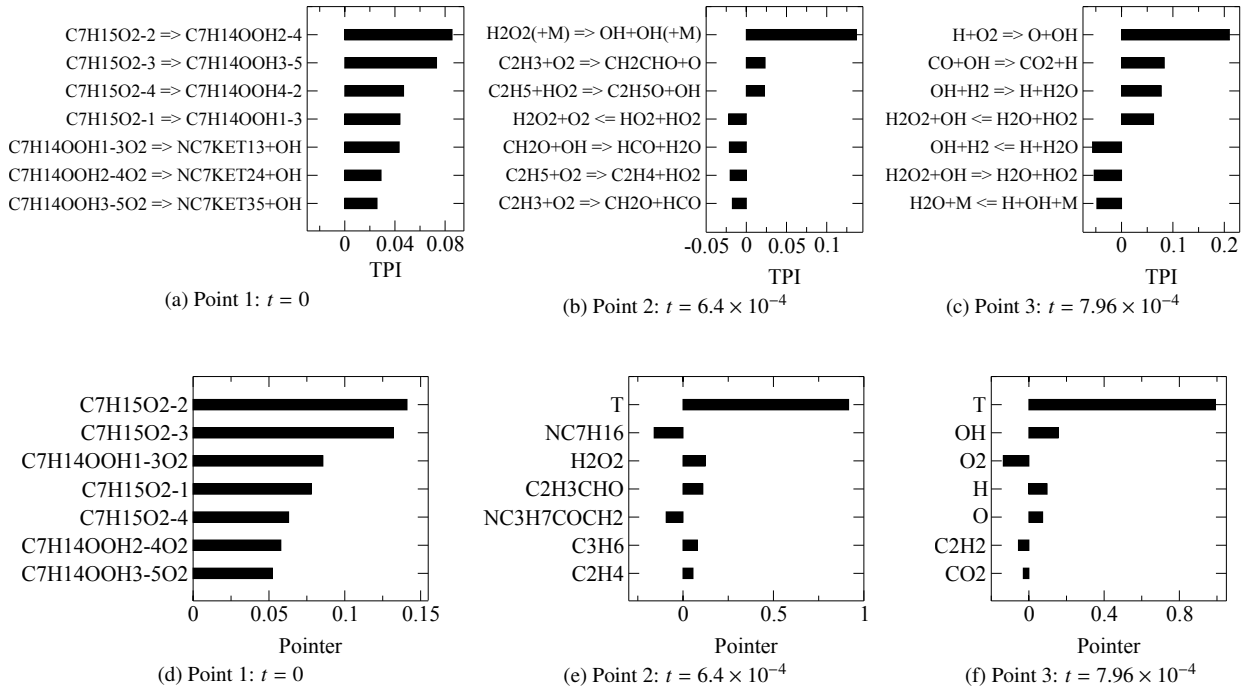

Figure 2: Top: the reactions with the largest Time scale Participation Indices (TPI). Bottom: the species with the largest CSP Pointers (Po) at the three selected points.

reaction is highly endothermic, which explains the reason why it doesn't proceed rapidly at low temperatures. The next two reactions with the largest TPI are $OH + H_2 \rightarrow H + H_2O$ and $CO + OH \rightarrow CO_2 + H$, which are both highly exothermic. Besides temperature, CSP Pointer, at point P_3, identifies species that are involved as reactants in the most significant reactions for the development of $\tau_{e,f}$.

Conclusions

Algorithmic asymptotic analysis was employed in order to identify the reactions that promote or oppose the generation of the explosive time scales that characterizes the homogeneous adiabatic autoignition of a *n*-heptane/air stoichiometric mixture at constant volume, for initial conditions of $p_0 = 30$ atm and $T_0 = 800$ K, which are of relevance to practical devices.

For the two stage auto-ignition process, it was shown

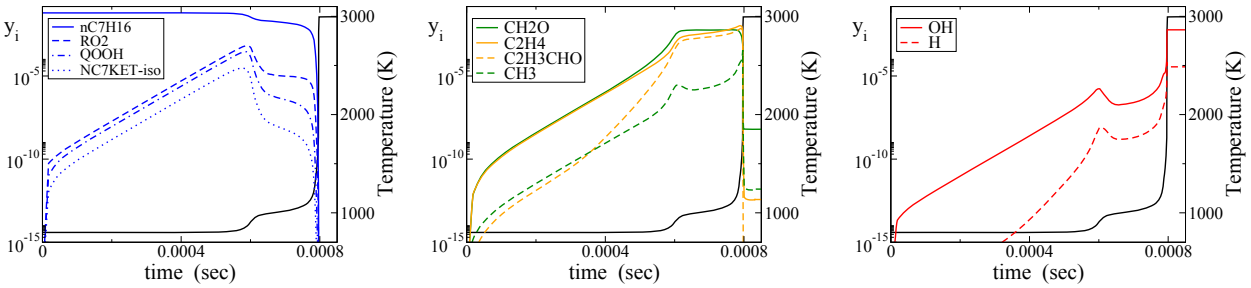

(a) heptane chemistry (b) ethyl/methyl chemistry (c) hydrogen chemistry

Figure 3: The evolution with time of the temperature and of selected species' mass fraction during the homogeneous autoignition process. The groups of species' mass fractions where selected according to the TPI and Pointer results and represent all the stages of the process. p_0 = 30 atm, T_0 = 800 K and ϕ = 1.

that as the process evolves, the nature of the reactions related to the characteristic explosive time scale evolves as well. It was shown that in the period that leads to the first stage, the reactions promoting $\tau_{e,f}$ are heptane isomerization reactions, such as intramolecular isomerization reactions of RO_2 isomers to $QOOH$ isomers and reactions of peroxyalkylhydroperoxides ($QOOH - O_2$) forming ketohyperoxides.

Right behind the first stage, $\tau_{e,f}$ is mainly due to the chain branching reaction $H_2O_2(+M) \rightarrow OH + OH(+M)$. As expected, the temperature starts been identified as the dominant variable for the mode that relates to $\tau_{e,f}$.

The second stage is characterized by reactions that relate to the hydrogen chemistry. The reaction contributing the most to $\tau_{e,f}$ is the chain branching reaction $H + O_2 \rightarrow O + OH$, while the highly exothermic reactions $OH + H_2 \rightarrow H + H_2O$ and $CO + OH \rightarrow CO_2 + H$ follow.

The reactions that relate to the evolution of the fast explosive time scale in each stage agree with the results of the existing literature. A reasonable extension of this work is to investigate the influence of various initial temperatures, pressures and mixture composition. Additionally, it would be interesting to investigate the effects of various additives in the initial mixture.

Acknowledgments

The work of DMM and DAG has been supported by the European Union (European Social Fund - ESF) and Greek national funds through the Operational Program "Education and Lifelong Learning" of the National Strategic Reference Framework (NSRF) - Research Funding Program: "ARISTEIA".

References

Diamantis, D., Kyritsis, D., Goussis, D. A., 2009. Two stage ignition of n-heptane: Identifying the chemistry setting the explosive time scales. In: 2nd Intl. Conference in Model Reduction in Reacting Flows.

Goussis, D., Skevis, G., 2005. Nitrogen chemistry controlling steps in methane-air premixed flames. In: Bathe, K. J. (Ed.), Computational Fluid and Solid Mechanics. Elsevier, Amsterdam, pp. 650–653.

Goussis, D. A., Najm, H. N., 2006. Model reduction and physical understanding of slowly oscillating processes: The circadian cycle. SIAM Multiscale Modeling and Simulation 5, 1297–1332.

Gupta, S., Im, H. G., Valorani, M., 2011. Classification of ignition regimes in HCCI combustion using computational singular perturbation. Proceedings of the Combustion Institute 33, 2991 – 2999.

Gupta, S., Im, H. G., Valorani, M., 2013. Analysis of n-heptane autoignition characteristics using computational singular perturbation. Proceedings of the Combustion Institute 34 (1), 1125 – 1133.

Kazakov, A., Chaos, M., Zhao, Z., Dryer, F. L., 2006. Computational singular perturbation analysis of two-stage ignition of large hydrocarbons. The Journal of Physical Chemistry A 110 (21), 7003–7009.

Lam, S. H., Goussis, D. A., 1988. Understanding complex chemical kinetics with Computational Singular Perturbation. Proceedings Combustion Institute. 22, 931–941.

Lam, S. H., Goussis, D. A., 1991. Conventional asymptotics and Computational Singular Perturbation for simplified kinetics modelling. In: Smooke, M. O. (Ed.), Reduced kinetic mechanisms and asymptotic approximations for methane-air flames. No. 384 in Springer Lecture Notes. Springer-Verlag, Berlin, pp. 227–242.

Lam, S. H., Goussis, D. A., 1994. CSP method for simplifying kinetics. International Journal of Chemical Kinetics 26 (4), 461–486.

Law, C. K., 2006. Combustion Physics. Cambridge University Press, New York.

Lee, J. C., Najm, H. N., Lefantzi, S., Ray, J., Frenklach, M., Valorani, M., Goussis, D., 2005. On chain branching and its role in homogeneous ignition and premixed flame propagation. In: Bathe, K. J. (Ed.), Computational Fluid and Solid Mechanics. Elsevier, Amsterdam, pp. 717–720.

Lu, T., Yoo, C., Chen, J., Law, C., 2010. Three-dimensional direct numerical simulation of a turbulent lifted hydrogen jet flame in heated coflow: a chemical explosive mode analysis. Journal of Fluid Mechanics 652, 45–64.

Mehl, M., Pitz, W. J., Westbrook, C. K., Curran, H. J., 2011. Kinetic modeling of gasoline surrogate components and mixtures under

engine conditions. Proceedings of the Combustion Institute 33 (1), 193 – 200.

n-heptane, 2012. https://www-pls.llnl.gov/?url=science_and_technology-chemistry-combustion-n_heptane_version_3.

Najm, H. N., Valorani, M., Goussis, D. A., Prager, J., 2010. Analysis of methane-air edge flame structure. Combustion Theory and Modelling 14 (2), 257–294.

Peters, N., Paczko, G., Seiser, R., Seshadri, K., 2002. Temperature cross-over and non-thermal runaway at two-stage ignition of n-heptane. Combust. Flame 128, 38–59.

Sanchez, A. L., Linan, A., Williams, F. A., 1997. A WKB analysis of radical growth in the hydrogen-air mixing layer. J. Eng. Math. 31, 19–130.

Shan, R., Yoo, C. S., Chen, J. H., Lu, T., 2012. Computational diagnostics for n-heptane flames with chemical explosive mode analysis. Combustion and Flame 159 (10), 3119 – 3127.

Trevino, C., 1989. Ignition phenomena in H2-O2 mixtures. Prog. Aeronaut. Astronaut. 131, 19–43.

Williams, F. A., 1985. Combustion Theory. The Benjamin/Cummings Publ. Co., Menlo Park, CA.

Yoo, C. S., Lu, T., Chen, J. H., Law, C. K., 2011. Direct numerical simulations of ignition of a lean n-heptane/air mixture with temperature inhomogeneities at constant volume: Parametric study. Combustion and Flame 158 (9), 1727 – 1741.